International Journal of Computing and Digital Systems
ISSN (2210-142X)
Int. J. Com. Dig. Sys. 14, No.1 (Sep-2023)

http://dx.doi.org/10.12785/ijcds/140155

Improvements in Sparse Array Based Beamformer via Additional Constraints

Diksha Thakur[1], Vikas Baghel[2] and Salman Raju Talluri[3]

[1]*Electronics and Communication Engneering,JUIT, Waknaghat, India*
[2]*Electronics and Communication Engneering,JUIT, Waknaghat, India*
[3]*Electronics and Communication Engneering,JUIT, Waknaghat, India*

Received 10 Jul. 2022, Revised 22 May 2023, Accepted 31 Jul. 2023, Published 01 Sep. 2023

Abstract: This paper presents the improvements that can be achieved through the additional constraints in the design of highly sparse arrays beamforming. The design of a highly sparse array beamformer is an optimization problem of multivariable functions and its performance depends on the given conditions. For a uniform linear array (ULA), the Output Signal to Noise Ratio (OSINR) is a linear function of antenna elements of the array. However, this linearity is not consistent in various antenna array environments. This deviation can be minimized by selecting an optimal sparse array with a lesser number of elements than that are actually required by an ULA. In this paper, a two-step procedure has been presented to find an optimal solution for designing a highly sparse antenna array beamformer with sidelobe control. Furthermore, to avoid the grating lobes and minimize the mutual coupling between the elements an additional degree of freedom in the form of separation between antenna elements is added to the optimization problem. Simulations results provided in the paper reveals that sparse arrays with the additional conditions are better in comparison with the arrays without constraints in terms of sidelobe level, grating lobes and mutual coupling.

Keywords:adaptive beamforming, sparse array, output signal to noise ratio, beampattern, sidelobe control.

I. Introduction

Adaptive beamforming is a key technology of array signal processing that is used to receive the signal of interest and counteracting interfering signals simultaneously. It has been widely employed in diverse fields such as wireless communication, satellite navigation, radar, sonar, cognitive radio, etc. [1]. A well known classical adaptive beamformer was proposed by Capon, named as minimum variance distortionless beamformer (MVDR)[2]. Various classical, as well as state of the art beamformers, have been mostly confined to the case of ULA, but to reduce the complexity of a system, non-uniform arrays and sparse arrays can be used instead of ULA [3], [4], [5]. Sparse arrays are created by choosing some antenna elements from the entire antenna array and only the chosen elements are used for further computation. The antenna elements of the sparse array are chosen to meet a certain objective. OSINR is an important metric to evaluate the performance of a beamformer and it is a function of the array configuration [6]. In the literature, various sparse array configurations were designed for different objectives such as beamwidth control, sidelobe control, OSINR maximization, etc. [7], [8], [9], [10], [11]. In [11], [12], the antenna elements were selected to maximize the OSINR. Though the optimized array configuration provided the maximum SINR but not able to control the sidelobes. High sidelobes were seen in the beampattern obtained from the optimal configuration. Hence, to enhance the performance of beamformers in the interference active environment, sidelobes should be controlled along with maximizing the OSINR. In recent years, various approaches have been developed for suppressing the sidelobes [13], [14], [15], [16], [17], [18]. But these algorithms were applied to linear arrays and can only suppress the sidelobes. The author of [19] had provided a formulation for sparse array designing which can suppress sidelobes but 70% elements of the full array were used in the proposed sparse array configuration. OSINR for a uniform linear array is not a linear function of the number of antenna elements for some specific environments and this motivates us to improve the linearity in sparse arrays. This can be further improved by adding additional constraints and degree of freedom. Apart from this, the control on the sidelobes has been given less importance so far by the researchers and this paper presents a slightly improved solution to beamforming with additional constraints. In this work, firstly a highly sparse array is designed for maximizing the OSINR then optimal weight vector with additional constraints to control

E-mail address: diksha.thakur18@gmail.com, dr.vikasbaghel@gmail.com, salmanraj7@gmail.com

sidelobe level is calculated. Finally, to avoid the grating lobes and minimize the mutual coupling between the elements, an additional degree of freedom as the distance between antenna elements in the array is added to the proposed optimization problem. This paper is organized in the following manner. Section 2 presents the mathematical formulation of the Minimum Variance Distortionless Response (MVDR) beamformer. The reformulation of MVDR beamformer with regards to sparse arrays along with mathematical formulation of additional constraints in the reformulated MVDR beamformer and distance variations are also done in this section. Section 3 presents the numerical simulations for the reformulations mentioned in section 2. Finally, section 4 presents the conclusions of the numerical simulations and the future scope of this analysis.

II. Signal Model and Problem Formulation

A. Signal Model

It is considered that P number of signals are impinging the array of M antenna elements and the received signals can be represented as Eq.1. These P signals can be split into interference signals and desired signals. Eq. 1 is indicating one desired signal impinging at angle of θ_o and $P-1$ interfering signals impinging at ϕ_i for $i=1$ to $i=P-1$. At any particular time instant t, the received signals at the particular antenna element can be written as

$$\boldsymbol{x}(t) = s_o(t)\boldsymbol{a}(\theta_o) + \sum_{i=1}^{P-1} s_i(t)\boldsymbol{a}(\phi_i) + \boldsymbol{n}(t) \tag{1}$$

where $s_o(t)$ denotes the signal of interest (SOI) and $s_i(t)$ is the interference signal. Along with SOI and interference, noise is also received at the elements and is denoted as $\boldsymbol{n}(t)$. The SOI and interference signals are incident from θ_o and $[\phi_1, ..., \phi_{P-1}]$ directions on the antenna array. The steering vectors of SOI and interference signal are denoted as $\boldsymbol{a}(\theta_o)$ and $\boldsymbol{a}(\phi_i)$, respectively. The covariance matrix $\hat{\boldsymbol{R}}$ is depicted in Eq. 2 that is based on theory is derived by adding the covariance matrix of the SOI and the covariance matrix of the interference and noise

$$\hat{\boldsymbol{R}} = \boldsymbol{R}_s + \boldsymbol{R}_{i+n} = \sigma_0^2\boldsymbol{a}(\theta_0)\boldsymbol{a}(\theta_0)^H + \sum_{i=1}^{P-1}\sigma_i^2\boldsymbol{a}(\phi_i)\boldsymbol{a}(\phi_i)^H + \sigma_n^2\boldsymbol{I} \tag{2}$$

where σ_0^2 , σ_i^2 and σ_n^2 are the SOI's power, i^{th} interference signal power and noise power respectively. In practice, the covariance matrix is determined from received samples on the antenna elements and for N_s samples it can be expressed as

$$\boldsymbol{R} = \frac{1}{N_s}\sum_{t=1}^{N_s}\boldsymbol{x}(t)\boldsymbol{x}^H(t) \tag{3}$$

The output of the adaptive beamformer is expressed as

$$\boldsymbol{y}(t) = \boldsymbol{w}^H\boldsymbol{x}(t) \tag{4}$$

where $\boldsymbol{w}$ is the antenna weight vector that is used to achieve beamforming i.e more energy is directed towards the desired signal and less or no energy towards the interference direction. In beamformer applications, it is required to minimize the noise and interference power to maximize the OSINR. The mathematical formulation for this maximization can be formulated as in Eq. 5 which is very well known and referred to as standard Capon beamformer (SCB).

$$min\ \ \boldsymbol{w}^H\boldsymbol{R}\boldsymbol{w} \qquad s.t. \quad \boldsymbol{w}^H\boldsymbol{a}(\theta_0) = 1 \tag{5}$$

Lagrange multiplier is utilized to simplify the Eq. 5 and the final result is depicted in Eq. 6.

$$\boldsymbol{w} = \frac{\boldsymbol{R}^{-1}\boldsymbol{a}(\theta_0)}{\boldsymbol{a}(\theta_0)^H\boldsymbol{R}^{-1}\boldsymbol{a}(\theta_0)} \tag{6}$$

Eq. 5 is used generally in uniform linear arrays and the same can be used even in sparse arrays if the steering vectors are known in advance. The steering vectors are primarily decided by the location of the antenna elements. MVDR beamformer can also be extended to sparse arrays by modifying the steering vectors according to the locations of the antenna elements. Here the main difference is the reduction in the dimensions of the steering vectors.

B. Improvements in standard Capon beamformer

The standard Capon optimization problem specified in Eq. 5 has been modified and reformulated in order to have multiple constraints in the optimized beampattern that will be equally applicable to the sparse arrays. Eq. 5 can be used for uniform linear arrays and non-uniform linear arrays. Since the emphasis of this paper is on the analysis of sparse arrays, sparse arrays are designed by maximizing the OSINR. In order to control the sidelobe levels while maximizing the OSINR, the additional constraint has been placed on the standard minimization problem. The additional constraints are placed on the region of interest (ROI) that includes he entire beampattern region except main lobe region. Let the ROI includes the angles ranges from $[\psi_1....\psi_2] \cup [\psi_3....\psi_4]$and $\boldsymbol{a}(ROI)$ is the respective steering vector. Now, a matrix of steering vectors $\boldsymbol{A}_{ROI}$ is formed that contains steering vectors for every angle of ROI. To control the sidelobe level, the response of ROI is constrained to the specified value ϵ. This problem has been modified and formulated as

$$\begin{aligned} &\min_{w} \qquad \boldsymbol{w}^H\boldsymbol{R}\boldsymbol{w} \\ &\quad subject\ to \\ &\quad \boldsymbol{w}^H\boldsymbol{a}(\theta_0) = 1 \\ &\quad \left|\boldsymbol{w}^{\mathbf{H}}\mathbf{A}_{\mathbf{ROI}}\right| <= \epsilon \end{aligned} \tag{7}$$

In general, the spacing between the antenna elements in arrays is considered to be half-wavelength. This is primarily to avoid the grating lobe. The grating lobe in the uniform linear arrays can be avoided by limiting the distance be-

tween the antenna elements to be less than half wavelength. Another important parameter in the antenna array is the mutual coupling between its elements. Due to the mutual coupling effect, the element responses interfere with each other. The effect of mutual coupling becomes noteworthy as the separation between the elements is decreased because more closer the elements are the more they interfere with each other. So, its effect can be minimized by increasing the inter-element spacing beyond half wavelength.

Now, to deal with grating lobes and mutual coupling effect, the optimization problem in Eq. 7 has been further modified to include another degree of freedom by adding the separation of elements d from a set of distances between the elements.To vary the distance a variable n is introduced in the formulation. n is an integer whose range is [0 4] such that the distance can be varied from 0.25λ to 0.75λ. This range is chosen such that the distance between elements is not so small which is not practically possible and not too large as the large distance between the elements makes the physical length of the array very large.

$$\begin{aligned} \min_{w} \quad & \boldsymbol{w}^H \boldsymbol{R} \boldsymbol{w} \\ & subject\ to \\ & \boldsymbol{w}^H \boldsymbol{a}(\theta_0) = 1 \\ & |\boldsymbol{w}^H \boldsymbol{A}_{ROI}| <= \epsilon \\ & d \in \left\{ 0.5\lambda \pm n\frac{\lambda}{16}, n = 0\ to\ 4 \right\} \end{aligned} \tag{8}$$

III. Numerical Simulations

A. Environment chosen for the Numerical simulations

In the numerical simulations three different interferences are considered which are occurring at three different frequencies f_{i1} = 2.9 GHz, f_{i2} = 3.1 GHz and f_{i3} = 3.2 GHz respectively. These three interferences impinging the array at angles ϕ_1 = 76, ϕ_2 = 83 and ϕ_3 = 101with powers of 20 dB , 20 dB and 30 dB respectively. It is assumed that the desired signal is coming at an angle of θ_o = 90 with frequency f_{SOI} = 3.0 GHz. The signal to noise ratio (SNR) is set to 0 dB.

B. ULA and Sparse arrays analysis for maximizing the OSINR

The OSINR for MVDR beamformer with optimal weight vector $\boldsymbol{w}$ given in Eq. 6 is expressed as

$$OSINR = \frac{\sigma_0^2 |\boldsymbol{w}^H \boldsymbol{a}(\theta_0)|^2}{\boldsymbol{w}^H \boldsymbol{R}_{i+n} \boldsymbol{w}} \tag{9}$$

Utilizing the weight vector $\boldsymbol{w}$ from Eq. 6 in Eq. 9, the OSINR can be written as

$$OSINR = ISNR \boldsymbol{a}(\theta_0)^H \boldsymbol{R}_a^{-1} \boldsymbol{a}(\theta_0) \tag{10}$$

where, the input signal to noise ratio (ISNR) and $\boldsymbol{R}_a$ are given as

$$ISNR = \frac{\sigma_o^2}{\sigma_n^2} \tag{11}$$

$$\boldsymbol{R}_a = \frac{\boldsymbol{R}_{i+n}}{\sigma_n^2} = I + \sigma_n^{-2} \boldsymbol{T} \boldsymbol{R}_i \boldsymbol{T}^H \tag{12}$$

where $\boldsymbol{T}$ is the interference array manifold matrix and $\boldsymbol{R}_i$ is the interference covariance matrix. The inverse of $\boldsymbol{R}_a$ can be evaluated by utilizing matrix inversion lemma

$$\boldsymbol{R}_a^{-1} = I - \boldsymbol{T}(\boldsymbol{R}_j + \boldsymbol{T}^H \boldsymbol{T})^{-1} \boldsymbol{T}^H \tag{13}$$

where $\boldsymbol{R}_j = \sigma_n^2 \boldsymbol{R}_i^{-1}$. The OSINR for different uniform linear arrays of size N for the above mentioned environment is obtained using the expression mentioned in Eq. 14.

$$OSINR = ISNR[N - \boldsymbol{a}(\theta_0) \boldsymbol{T}(\boldsymbol{R}_j + \boldsymbol{T}^H \boldsymbol{T})^{-1} \boldsymbol{T}^H \boldsymbol{a}(\theta_0)] \tag{14}$$

From the expression in Eq 14, it can be noticed that the variation of OSINR as a function of the number of elements is linear. To have more clarity, OSINR is evaluated by varying number of antenna elements in ULA. The number of elements in the array (N) are varied from N = 2 to N = 40 with half-wavelength spacing between them. The Fig. 1 and Fig. 2 display the actual and expected relationship between the OSINR and number of antenna elements. From where, it is observed that the OSINR is not linear for the given environment, and in fact, its deviation is more at lower number of elements. At N = 12 elements, the difference between the expected OSINR and obtained OSINR is about 3dB. Since this paper addresses the sparse arrays, this characteristic plays an important role in the selection of the number of antenna elements required to have better performance according to the existing environmental conditions.

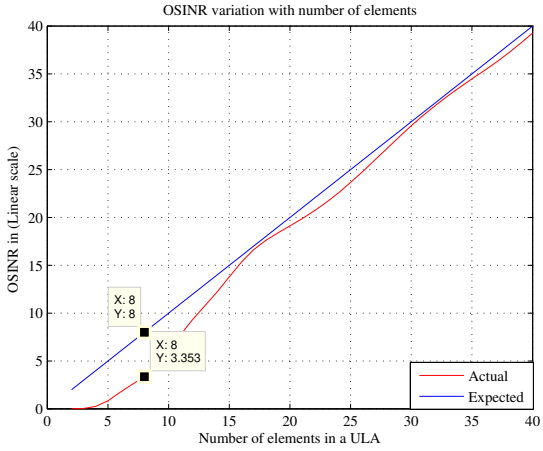

Figure 1. Variation of OSINR(linear) with number of elements

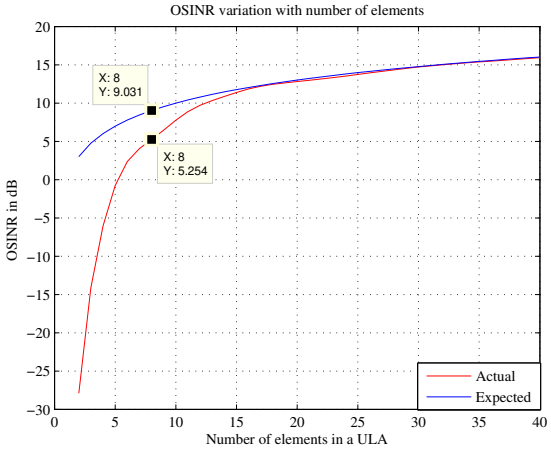

Figure 2. Variation of OSINR(dB) with number of elements

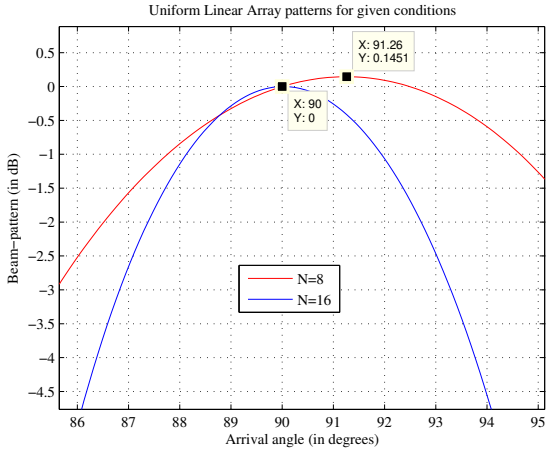

Figure 4. Beampatterns for N=8 and N=16(no shift) uniform linear arrays

In order to have the effect of selection of less number of elements in the uniform linear array, the patterns are obtained for two selections with reduced number of elements. The beampatterns obtained for $N = 8$ and $N = 16$ are displayed in Fig. 3. From this figure, it is clear that the uniform linear array may not work properly in the given environment. There is a shift in the main beam direction when number of antenna elements is reduced to 8 that is clear from the Fig. 4. In order to have a comparison with [11] OSINR and validate the numerical simulations, the number of elements in a uniform linear array has been chosen as $N = 16$.

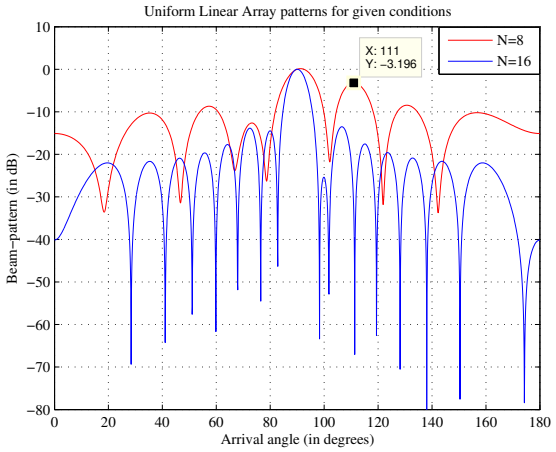

Figure 3. Beampatterns for N=8 and N=16 uniform linear arrays

C. Design of optimal sparse array structure/configuration

Since the uniform linear arrays are not able to provide a reasonable beampattern and even the OSINR, the sparse arrays have been explored and the OSINR for optimal sparse arrays from $N = 8$ to $N = 16$ has been presented in section 3.4. In other words, the sparsity has been observed from 50% to full array. It is observed that for each sparsity, there is an optimal location vector of the antenna array for each K. The OSINR for these optimal arrays for each K has been observed and the OSINR in this case varies linearly in comparison with the full uniform linear arrays of size K. The optimal array structure/ configuration is determined on the basis of OSINR and the procedure is explained is as follows:

1) Select K number of antenna elements from the total antenna elements in the array (N).
2) Search all possible combinations C(N,K) and calculate the OSINR using Eq. 14 for all possible combinations.
3) Finally, the configuration/ antenna structure that provides maximum OSINR is selected and called as optimal configuration.

Now, sparse arrays are constructed by selecting K=8,9 antenna elements from N=16 elements. The OSINR is evaluated for all possible combinations of C(16,8) and C(16,9). The OSINR of each possible configuration for K=8 and K=9 is depicted in Fig. 5. From the figure it is observed that there is a difference of approximately 9dB is the OSINR of best and worst array configuration. The sparse array configurations with maximum OSINR for K=8 and K=9 are as follows:

$$[1 \quad 3 \quad 6 \quad 7 \quad 9 \quad 11 \quad 13 \quad 16] \qquad K = 8 \qquad (15)$$

$$[1 \quad 4 \quad 5 \quad 7 \quad 9 \quad 10 \quad 11 \quad 14 \quad 16] \qquad K = 9 \qquad (16)$$

Now, beampatterns are obtained with best array configurations given in Eq. 15 and 16. The beampatterns for $K = 8$ and $K = 9$ are represented in Fig. 6. The weights for each

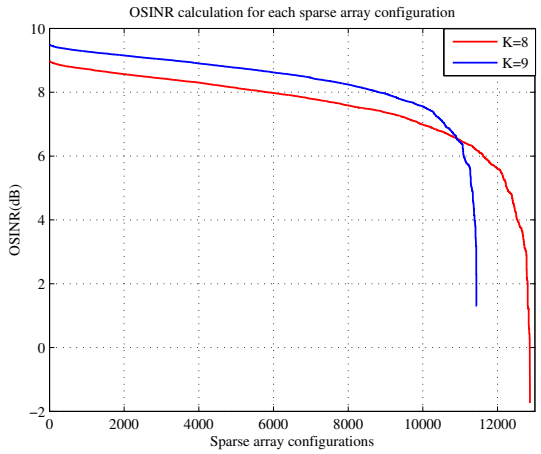

Figure 5. OSINR of all sparse array configurations for K=8

of the best sparse array has been obtained and the antenna beampattern is observed for each sparsity. It is observed that the highly sparse arrays are producing higher sidelobe levels near the outside of the interested region. From Fig. 6, it is

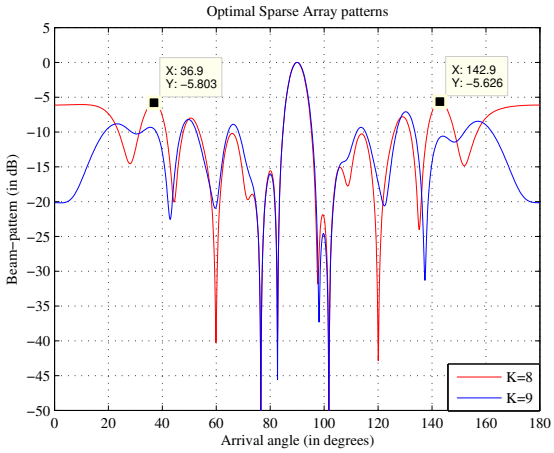

Figure 6. Optimal beampatterns for K=8 and K=9

also observed that the sidelobes near the main beam are above -10 dB, and in some cases, it is required to have the sidelobe levels lower than -10 dB depending on the requirement. Hence, these additional constraints have been placed on the beampattern to lower the sidelobe levels. These conditions are chosen such that from 30^o to 150^o with an increment of 5^o by leaving the interference and main beam angles. These angles are $[30^o\ 70^o] \cup [110^o\ 150^o\ ]$.

The additionally constrained patterns have been represented in Fig. 7 for $K = 8$ and $K = 9$. From this figure, it is observed that $K = 8$ is able to meet the required conditions of having less than -10 dB near the main beam direction even though the beampattern is dominant at the far away angles from the main beam. This observation has also suggested to introduce another degree of freedom in terms of distance as the dominant side lobe is occurring at the far away angles from the main beam. This can be considered as the emergence of the grating lobe. The antenna elements in the array are separated by the distance of half wavelength and this distance is mainly chosen to avoid the grating lobe. Since the sparsity considered in this paper is emphasized on sparsity around 50%, this spacing condition to avoid grating lobe can be relaxed. The grating lobe in the uniform linear arrays can be avoided by restricting the distance between the antenna elements to be less than half wavelength. This can be relaxed in sparse arrays as the distance between the elements can be varied depending on the selection of the antenna positions.

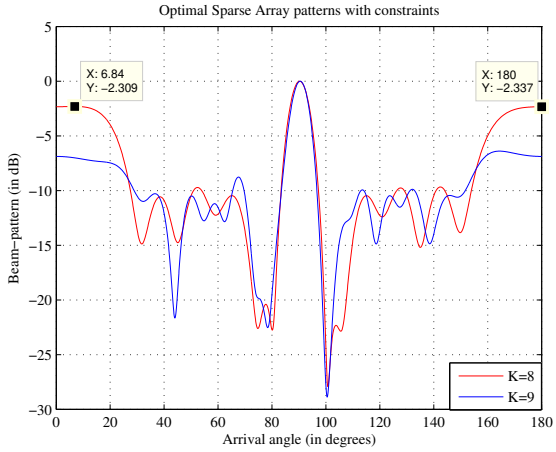

Figure 7. Additionally Constrained Optimal beampatterns for K=8 and K= 9

D. Analysis with Distance Variations

In order to observe the variation of beampattern with the distance between the antenna elements in the sparse array, few numerical simulations have been carried out by varying the distance between the elements. The separations have been considered to be multiples of $\lambda/16$ (0.0625λ) from 0.3750λ to 0.6250λ. The other samples with reasonable patterns are maintained at distances of 0.4375λ, 0.5000λ, and 0.5625λ. Fig. 8 represent the sparse arrays with $K = 8$ for different element spacing and from this, it is observed that at a distance of 0.4375λ, the pattern is much flat for the entire visible region except the main beam. The zoomed version of the main beams is given in Fig. 9 from where it can be seen that d=0.4375λ is the only distance to produce main beam towards the exact DOA of SOI. Fig. 10 represent the similar pattern for $K = 9$. In comparison with $K = 8$, the sidelobe levels outside the interested region

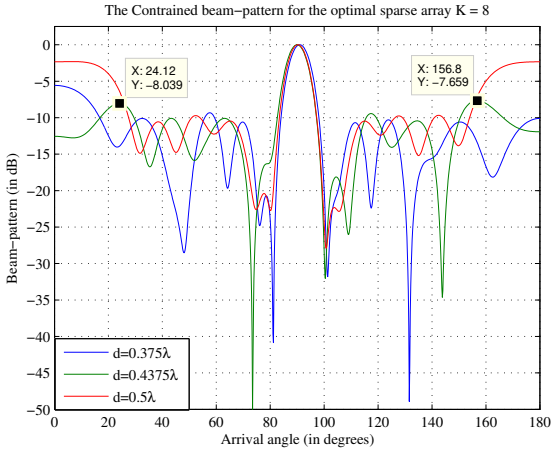

Figure 8. Beampatterns of optimal sparse arrays with K=8

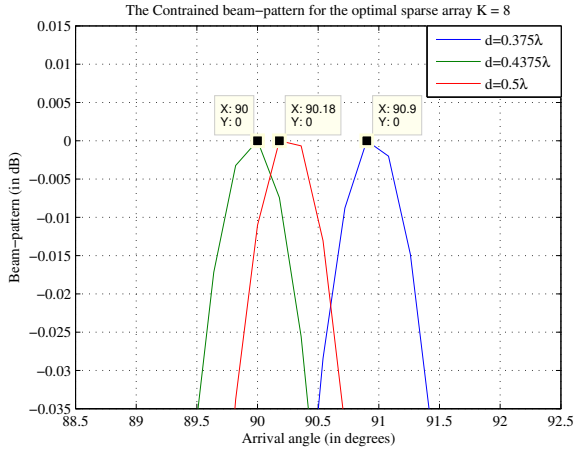

Figure 9. Beam-patterns of optimal sparse arrays with K=8

are reasonably suppressed by approximately 1dB for all the distances. However, for a distance of 0.5625λ, the pattern appears to be good in comparison with the other distances. A comparison of constrained and unconstrained beampatterns for a distance of $0.4375\lambda$is made and the corresponding results are shown in Fig. 11 and Fig. 12 respectively. From the figures it is observed that the better optimal solution is with $K = 8$ as the pattern for $K = 8$ is improved response as compared to the unconstrained response.

A similar numerical analysis has been performed for expanded lengths. Fig. 13 and Fig. 14 represent the beampatterns for larger separations for $K = 9$ only. Here $K = 8$ is not able to provide a solution meeting all the requirements and has an infeasible solution with $K = 8$. From these figures, it is observed that the beampattern is distorted for higher values of separation between the elements.

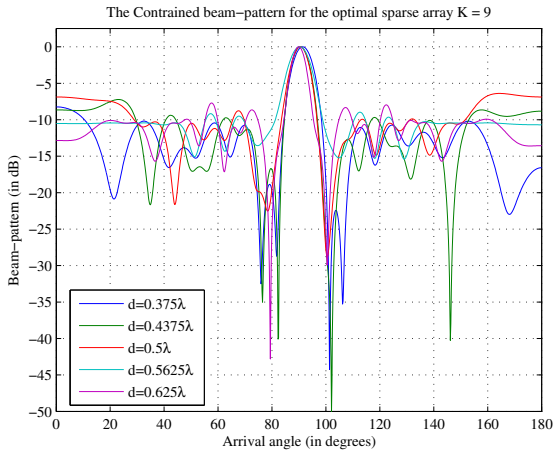

Figure 10. Beam-patterns of optimal sparse arrays with $K = 9$

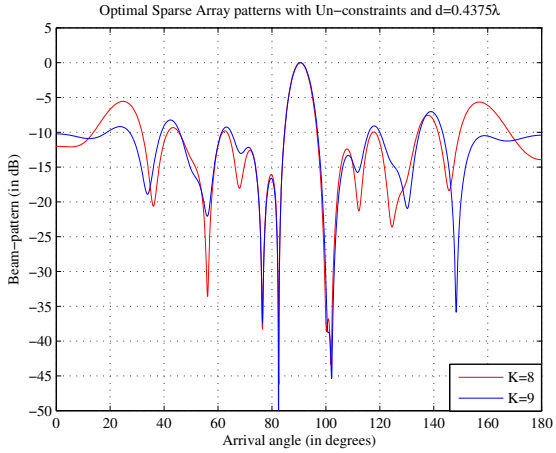

Figure 11. Reduced distance of separation with $d = 0.4375\lambda$ for $K = 8$ and $K = 9$

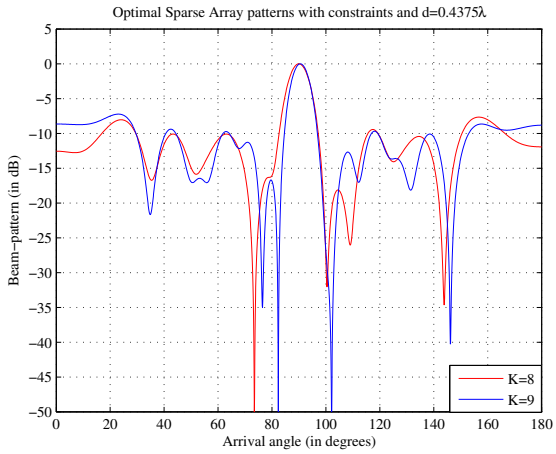

Figure 12. Reduced distance of separation with $d = 0.4375\lambda K = 8$ and $K = 9$

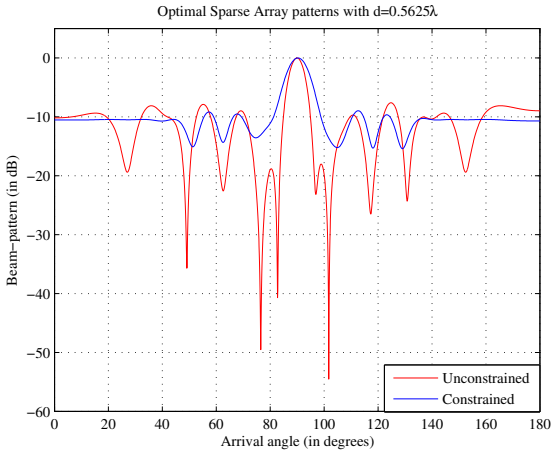

Figure 13. Expanded distance of separation with $d = 0.5625\lambda$ and $K = 9$

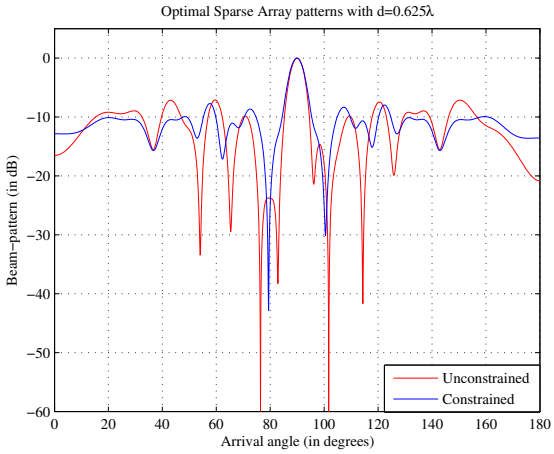

Figure 14. Expanded distance of separation with $d = 0.6250\lambda$ and $K = 9$

From these numerical simulations, it has been validated that the improvement in the beampattern can be obtained by using the sparse arrays with additional constraints.

E. OSINR observations

To evaluate the performance of sparse arrays OSINR is calculated by varying the number of antenna elements from $N = 8$ to $N = 16$ and the results are shown in Fig. 15. From the figure, it is clearly visible that the OSINR of sparse array follows the expected OSINR whereas ULA is not able to provide the expected OSINR with less number of elements. In order to examine the effect of separation between the antenna elements on the OSINR, the distance is varied for two different scenarios. In the first case, the OSINR is calculated for distances of less than half wavelength and then the distances of more than half wavelength are considered. The simulation results for two different scenarios

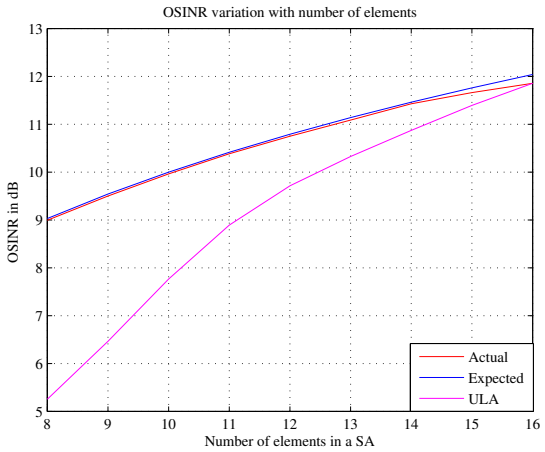

Figure 15. Comparison of OSINR of sparse arrays and ULAs

are depicted in Fig. 16 and Fig. 17. From the Fig. 16, it is

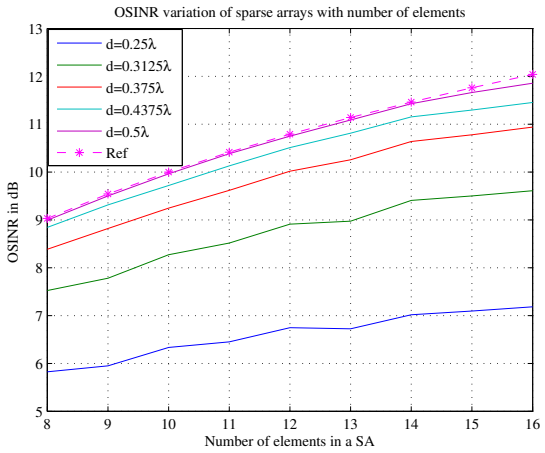

Figure 16. Variation of output SINR for sparse arrays with distance less than half wavelength

observed that as the distance between the antenna elements decreases beyond half wavelength the OSINR also decreases. Now, the effect of an increase in the distance after a half wavelength is also studied and it is observed from the Fig. 17 that with the increase in distance the OSINR decreases. The optimal distance in terms of best OSINR for both the scenarios is half wavelength only.

F. A step by step procedure to design an efficient sparse beamformer with an extra degree of freedom, distance between the elements.

The following procedure is outlined after few numerical simulations.

1) Obtain the best positions for the sparse array with uniform spacing of half wavelength between the elements.

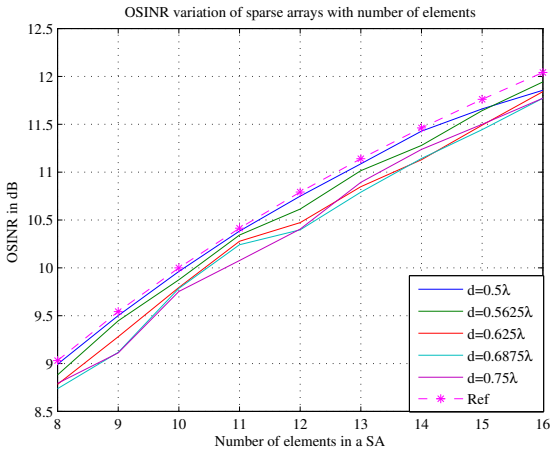

Figure 17. Variation of output SINR for sparse arrays with distance more than half wavelength

2) The incorporate additional constraints based on the environment of the antenna.
3) The constraints are supposed to be chosen that there is a reasonable grating lobe appears at the far away angles from the main beam. This can be considered to be back-lobe.
4) Finally with the above constraints, reduce the distance between the elements to obtain the best possible beam-pattern to maximize the OSINR while controlling the sidelobe levels.

It has also been observed that the linear search of $K = 8$ to $K = 16$ revealed that the first element and last element are always active in the best possible sparse arrays. This indicated that the physical length of the array has a say in deciding the maximum OSINR. The simulation has indicated that the same performance can be obtained with the reduced distance **(Compact sparse array)** by increasing the OSINR for a uniform linear array itself.

IV. Comparative analysis

A comparative study of various state-of-the-arts with the proposed method is depicted in Table I. The parameters taken for comparison are sparsity, SLL and OSINR. The method of [11] used only 50% of antenna array elements and is capable of suppressing the sidelobes but OSINR is less in comparison to the considered methods. The OSINR is improved in [12] at the cost of increased sidelobes with 57% of antenna elements.Furthermore, the method proposed in [19] is not able to suppress the sidelobes even though 70% of its antenna elements are used. In comparison, the proposed method utilized only 50% of antenna elements and improved OSINR by approximately 11% and 58% compared to [12] and [11], respectively. The proposed method also yields suppressed sidelobes in interested region, as the obtained SLL is less than −20dB. Therefore, the proposed array configuration is preferred over other methods for achieving good OSINR performance as well as for the lower sidelobes.

TABLE I. Comparative analysis of various methods.

Methods ↓	Sparsity	SLL	OSINR
X.Wang et al. [11]	50%	−15dB	7.5dB
X.Wang et al. [12]	57%	above −10dB	10.68dB
Z.Zheng et al. [19]	70%	above −10dB	NA
Proposed work	50%	below −20dB	11.89dB

V. Conclusion

The numerical simulations presented in this paper indicate that for sparse arrays, OSINR, along with sidelobe control over the region of interest, can be further improved by properly defining the additional constraints. The locations of the optimal sparse arrays have been obtained by a linear search. Along with this, the distance between the antenna elements has been used as another degree of freedom to control the sidelobe levels. From the analysis, it is presented that with the introduction of additional carefully designed constraints, an optimal sparse array can be designed to meet the stringent specifications for an antenna array. The procedure to design an efficient sparse array has been formulated from the careful observation of numerical results. This work can be further improved by using an optimal searching algorithm for optimal sparse array configuration instead of linear search.

References

[1] S. Applebaum, “Adaptive arrays,” *IEEE Transactions on Antennas and Propagation*, vol. 24, no. 5, pp. 585–598, 1976.

[2] J. Capon, “High-resolution frequency-wavenumber spectrum analysis,” *Proceedings of the IEEE*, vol. 57, no. 8, pp. 1408–1418, 1969.

[3] A. F. Molisch and M. Z. Win, “Mimo systems with antenna selection,” *IEEE microwave magazine*, vol. 5, no. 1, pp. 46–56, 2004.

[4] S. Sanayei and A. Nosratinia, “Antenna selection in mimo systems,” *IEEE Communications magazine*, vol. 42, no. 10, pp. 68–73, 2004.

[5] S. R. Shebert, M. G. Amin, B. H. Kirk, and R. M. Buehrer, “Multi-signal classification using deep learning and sparse arrays,” *2022 IEEE Military Communications Conference (MILCOM)*, pp. 1–6, 2022.

[6] M. Wax and Y. Anu, “Performance analysis of the minimum variance beamformer,” *IEEE Transactions on Signal Processing*, vol. 44, no. 4, pp. 928–937, 1996.

[7] A. Gorokhov, D. A. Gore, and A. J. Paulraj, “Receive antenna selection for mimo spatial multiplexing: theory and algorithms,” *IEEE Transactions on signal processing*, vol. 51, no. 11, pp. 2796–2807, 2003.

[8] S. E. Nai, W. Ser, Z. L. Yu, and H. Chen, “Beampattern synthesis for linear and planar arrays with antenna selection by convex optimization,” *IEEE Transactions on Antennas and Propagation*, vol. 58, no. 12, pp. 3923–3930, 2010.

[9] X. Wang, M. S. Greco, and F. Gini, "Adaptive sparse array beamformer design by regularized complementary antenna switching," *IEEE Transactions on Signal Processing*, vol. 69, pp. 2302–2315, 2021.

[10] N. B. Mehta, S. Kashyap, and A. F. Molisch, "Antenna selection in lte: From motivation to specification," *IEEE Communications Magazine*, vol. 50, no. 10, pp. 144–150, 2012.

[11] X. Wang, M. Amin, and X. Wang, "Robust sparse array design for adaptive beamforming against doa mismatch," *Signal Processing*, vol. 146, pp. 41–49, 2018.

[12] X. Wang, M. Amin, and X. Cao, "Analysis and design of optimum sparse array configurations for adaptive beamforming," *IEEE Transactions on Signal Processing*, vol. 66, no. 2, pp. 340–351, 2017.

[13] K. Yang, Z. Zhao, X. Zhu, and Q. H. Liu, "Robust adaptive beamforming with low sidelobe levels," *2013 IEEE Antennas and Propagation Society International Symposium (APSURSI)*, pp. 872–873, 2013.

[14] A. Sharma and S. Mathur, "A novel adaptive beamforming with reduced side lobe level using gsa," *COMPEL-The international journal for computation and mathematics in electrical and electronic engineering*, 2018.

[15] P. Li, L. Wang, Z. Sun, C. Bian, D. Zhao, R. Xie, and Y. Rui, "Robust adaptive beamforming with sidelobe controlled based on improved objective function," *2019 International Applied Computational Electromagnetics Society Symposium-China (ACES)*, vol. 1, pp. 1–2, 2019.

[16] I. P. Gravas, Z. D. Zaharis, T. V. Yioultsis, P. I. Lazaridis, and T. D. Xenos, "Adaptive beamforming with sidelobe suppression by placing extra radiation pattern nulls," *IEEE Transactions on Antennas and Propagation*, vol. 67, no. 6, pp. 3853–3862, 2019.

[17] M. Zhou, X. Ma, P. Shen, and W. Sheng, "Weighted subspace-constrained adaptive beamforming for sidelobe control," *IEEE Communications Letters*, vol. 23, no. 3, pp. 458–461, 2019.

[18] D. Thakur, V. Baghel, and S. R. Talluri, "A dual beam adaptive beamforming algorithm with sidelobe suppression," *Measurement: Sensors*, vol. 24, p. 100514, 2022.

[19] Z. Zheng, Y. Fu, W.-Q. Wang, and H. C. So, "Sparse array design for adaptive beamforming via semidefinite relaxation," *IEEE Signal Processing Letters*, vol. 27, pp. 925–929, 2020.

Authors' Biography

Diksha Thakur received the B.Tech degree in Electronics and Communication Engineering from PTU in 2014 and the M.Tech degree in Electronics and Communication Engineering from JUIT, Solan in 2018. Since July 2018, she has been working towards the Ph.D degree at JUIT, Solan. Her research interests include array signal processing and microwave engineering

Dr. Vikas Baghel received his Ph.D. degree in Radar Signal Processing from IIT Bhubaneswar in 2014, M.Tech degree in Telematics and Signal Processing from NIT Rourkela in 2009 and B.Tech degree in Electronics and Communication Engineering from UPTU Lucknow in 2007. He is presently working as Assistant Professor (Sr. Grade) in the Department of Electronics and Communication Engineering with Jaypee University of Information Technology, Waknaghat. His broad area of research interest is Signal Processing with specialization in Radar Signal Processing. He was the recipient of Commonwealth Fellowship from DFAIT, Canada.

Dr. Salman Raju Talluri received his Ph.D. degree from JUIT, Solan in 2016, M.Tech from IITK in 2009 and B.E. in Electronics and Communication Engineering from Anil Neerukonda Institute of Technology & Sciences in 2006. He has worked with Astra Microwave Products Limited, HYD and Tejas Networks, Bangalore for one year each. He is presently working as Assistant Professor (Sr. Grade) in the Department of Electronics and Communication Engineering with Jaypee University of Information Technology, Waknaghat. He has published many research papers in peer reviewed reputed international journals. His areas of interest include microwave engineering and antenna array.